An improved EEHEMT model for kink effect on AlGaN/GaN HEMT*

Cao Meng-Yi(曹梦逸)[a], Lu Yang(卢 阳)[a], Wei Jia-Xing(魏家行)[b], Chen Yong-He(陈永和)[a], Li Wei-Jun(李卫军)[b], Zheng Jia-Xin(郑佳欣)[a], Ma Xiao-Hua(马晓华)[a,b,†], and Hao Yue(郝 跃)[a]

[a] *Key Laboratory for Wide Band-Gap Semiconductor Materials and Devices, School of Microelectronics, Xidian University, Xi'an* 710071, *China*
[b] *School of Advanced Materials and Nanotechnology, Xidian University, Xi'an* 710071, *China*

(Received 30 November 2013; revised manuscript received 23 January 2014; published online 10 June 2014)

In this paper, a new current expression based on both the direct currect (DC) characteristics of the AlGaN/GaN high election mobility transistor (HEMT) and the hyperbolic tangent function tanh is proposed, by which we can describe the kink effect of the AlGaN/GaN HEMT well. Then, an improved EEHEMT model including the proposed current expression is presented. The simulated and measured results of *I*–*V*, *S*-parameter, and radio frequency (RF) large-signal characteristics are compared for a self-developed on-wafer AlGaN/GaN HEMT with ten gate fingers each being 0.4-μm long and 125-μm wide (Such an AlGaN/GaN HEMT is denoted as AlGaN/GaN HEMT (10×125 μm)). The improved large signal model simulates the *I*–*V* characteristic much more accurately than the original one, and its transconductance and RF characteristics are also in excellent agreement with the measured data.

Keywords: AlGaN/GaN HEMT, kink effect, tanh, EEHEMT model

PACS: 72.20.Ht, 73.40.Kp, 73.61.Ey **DOI:** 10.1088/1674-1056/23/8/087201

1. Introduction

The AlGaN/GaN high electron mobility transistor (HEMT) has a very broad prospect in applications in the areas of high frequency,[1] high temperature,[2] and high power[3] due to its promising performance such as high breakdown field, high thermal conductivity, high saturated electron drift velocity, and high electron mobility. With the substrate of silicon carbide with excellent thermal properties, GaN HEMTs are optimal for high-power radio frequency (RF) applications. In recent years, GaN HEMTs with different structures, such as an enhancement mode (E-mode) HEMT[4] and metal–insulator–semiconductor (MIS) HEMT,[5] have been developed. Despite the continuous improvement of GaN HEMTs, the kink effect is still a key issue in research. The kink effect resulting from the shift in threshold voltage, appears as an increase of varying degrees in drain current in a certain drain/gate voltage range.[6] The drain voltage, which causes the kink effect, has a complicated relationship with the bias condition.[7] By using Matlab simulation, a semi-empirical model about the kink effect on AlGaN/GaN HEMT was established by Ma *et al.*[8]

The design of AlGaN/GaN HEMT-based power amplifiers requires a large signal model for the devices used. The accuracy of the model is a key factor that determines the results of the circuit and system design. Therefore, the study of the model of transistors is a basis for computer aided design (CAD) and the microwave circuit design. In past years, many large-signal models have been proposed to investigate the direct current (DC) and RF characteristics of the GaN HEMT. However, few of them are for the kink effect. The large-signal model including the kink effect is still under research.

In this paper, we propose a new current expression based both on the DC characteristic of the AlGaN/GaN HEMT and hyperbolic tangent function tanh to describe the kink effect of the device. Then we incorporate the current expression into the EEHEMT model, keeping the merits of the original model unchanged. This model for the kink effect is based on the testing data; in theory, it can be used for any type of AlGaN/GaN HEMT with a kink effect. The simulated and measured results of *I*–*V*, *S*-parameter, and RF large-signal characteristics are compared for a self-developed on-wafer AlGaN/GaN HEMT with a gate length of 0.4 μm and a gate width of 10×125 μm. The improved model simulates the kink effect accurately, while the simulated DC and RF characteristics are in excellent agreement with the measured data.

2. Extraction procedure

Figure 1 shows the proposed EEHEMT model for an AlGaN/GaN HEMT. The equivalent circuit contains both intrinsic and extrinsic elements. In this circuit, two quasi-static gate current sources, I_{gs} and I_{gd} and two quasi-static gate charge sources, Q_{gc} and Q_{gy}, are used to describe the condition and displacement currents.[9] The extrinsic elements are first extracted by the "cold-FET" technique. The pad capacitances

*Project supported by the National Natural Science Foundation of China (Grant No. 61334002), the Opening Project of Science and Technology on Reliability Physics and Application Technology of Electronic Component Laboratory (Grant No. ZHD201206), and the Program for New Century Excellent Talents in University (Grant No. NCET-12-0915).

†Corresponding author. E-mail: xhma@xidian.edu.cn

© 2014 Chinese Physical Society and IOP Publishing Ltd

C_{gp} and C_{dp} are determined from the cold pinch-off ($V_{ds} = 0$, V_{gs}<V_{th}) S-parameter, and the extrinsic resistances and inductances are extracted from the cold-forward ($V_{ds} = 0$, $V_{gs} = 2$ V) S-parameter following the process in Ref. [10]. After de-embedding the extracted extrinsic elements from the measured S-parameters, we obtain the intrinsic Y-parameter. By linear fitting under a certain bias condition, we obtain the values of the linear intrinsic elements.[10]

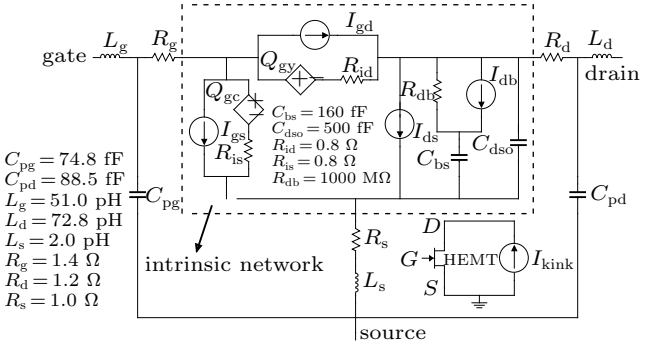


Fig. 1. Improved EEHEMT model for AlGaN/GaN HEMT including kink effect. The values of the extrinsic and linear intrinsic elements correspond to on-wafer AlGaN/GaN HEMT (10×125 μm).

In the extraction of DC parameters, we measure the I_{ds}–V_{gs} characteristic curve and calculate its first three derivatives. By fitting the measured g_m–V_{gs} curve, we obtain the values of the DC parameters Gmmax, V_{go}, V_{co}, V_{to}, Alpha, DELTGM, V_{ba}, and V_{bc} in the EEHEMT model. After the extraction of DC parameters, we extract the AC parameters. The extrinsic elements and linear intrinsic elements have been extracted above. In the EEHEMT model, the output capacitance is a constant C_{dso}. The gate–source and gate–drain capacitance vary with bias voltage. We measure S-parameters under different bias conditions and correspondingly extract C_{gs} and C_{gd}.[10] Then we fit the curves of C_{gs}–V_{gs} and C_{gs}–V_{gd} to obtain the values of C11o, C11th, Deltgs, Deltds, Vinfl, and Lambda. The C_{gd} is modeled by C12sat (input transcapacitance for V_{gs} = Vinfl and V_{ds} > Deltds) and Cgdsat (gate drain capacitance for V_{ds} > Deltds).

3. Model of kink effect

The kink effect is found in many types of semiconductor devices.[11] It results from the shift in threshold voltage. The phenomenon of the kink effect appears as an increase of varying degrees in the drain current in a certain drain/gate voltage range. When V_{gs} and V_{ds} vary in forward or reverse modes, the DC I–V curves will change slightly, which is ubiquitous in AlGaN/GaN HEMTs. In different sweep conditions, the kink effect area will exhibit a shift, but it is very tiny and can be neglected. Neither the speed nor step of the voltage sweeping has an effect on the DC curve. To describe the current variation, we propose a new expression for the drain current of the device. The new current expression is based on both the DC characteristics of the device and the hyperbolic tangent function tanh, and shown below

$$I_{dkink}(V_{gs}, V_{ds}) = \frac{\Delta I_d}{2} + \frac{\Delta I_d}{2} \cdot \tanh\left[\frac{\alpha \cdot (V_{ds} - V_{dkink})}{\Delta V_d/2}\right]. \quad (1)$$

Figure 2 shows the meanings of ΔI_d, ΔV_d, and V_{dkink} in Eq. (1). ΔI_d is the current increment caused by the kink effect. V_{dkink0} is the drain–source voltage where the kink effect starts to occur and V_{dkink1} is where the kink effect ends. V_{dkink} is the drain–source voltage where the drain current increases fastest in the kink effect area. I_{d0} and I_{d1} are the drain current at V_{dkink0} and V_{dkink1}, respectively. So, $\Delta I_d = I_{d1} - I_{d0}$ and $\Delta V_d = V_{dkink1} - V_{dkink0}$. In Eq. (1), α is a correction factor to optimize the simulation results.

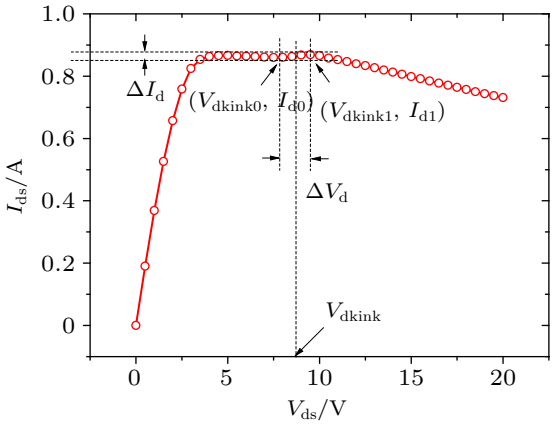


Fig. 2. (color online) Meanings of the parameters in the kink effect area.

To ascertain the domain of the kink effect, we take the first derivative of the drain current I_{ds} with respect to drain voltage V_{ds} according to the DC current curve. The domain of the kink effect can be determined by the two points at which the first derivative of I_{ds} with respect to V_{ds} is zero. Figure 3(a) shows the curves of the derivative of the drain current I_{ds} with respect to drain voltage V_{ds} under different gate bias voltages. From the curves, we can ascertain the domain of the kink effect and then obtain the values of V_{dkink0} and V_{dkink1} by reading the zero point. When the DC current is small, the first derivative is always larger than zero so that the starting voltage point is not obvious. We approximate the starting point where the first derivative of I_{ds} with respect to V_{ds} reaches the minimum value. By reading the voltages where the derivatives reach the maximum value in the kink effect range, we obtain the values of V_{dkink}.

Afterwards, ΔI_d, ΔV_d, and V_{dkink} shown in Fig. 2 can be determined immediately. Figures 3(b)–3(d) show the variations of ΔI_d, ΔV_d, and V_{dkink} with V_{gs}, respectively. According to the extracted parameters, we fit the curves of ΔI_d–V_{gs}, ΔV_d–V_{gs}, and V_{dkink}–V_{gs} by using second-order polynomials as shown below

$$\Delta I_d = a_I{}^* V_{gs}{}^2 + b_I{}^* V_{gs} + c_I, \quad (2)$$

$$\Delta V_d = a_v{}^* V_{gs}{}^2 + b_V{}^* V_{gs} + c_V, \quad (3)$$

$$V_{\rm dkink} = a_{\rm k}{}^{*}V_{\rm gs}{}^{2} + b_{\rm k}{}^{*}V_{\rm gs} + c_{\rm k}. \quad (4)$$

By substituting all these parameters into Eq. (1), we can calculate the value of $I_{\rm dkink}$. By subtracting $I_{\rm dkink}$ from the original simulated drain current and tuning the correction factor α, we can obtain the $I_{\rm ds}$ with the kink effect. To improve the DC *I–V* characteristics of the EEHEMT model, we add the kink effect model to the original large-signal model as figure 1 shows in advance design system (ADS).

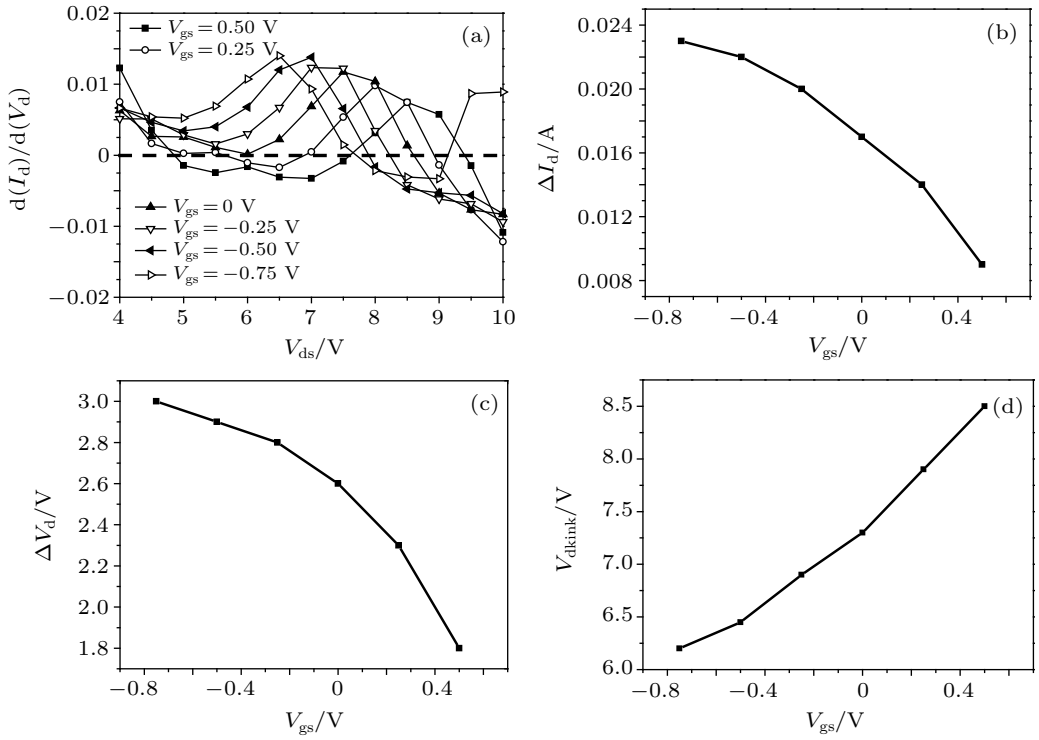


Fig. 3. Meanings of the parameters in the kink effect area.

4. Experimental verification

In order to validate the accuracy of the improved EEHEMT model, we implement it in ADS and then verify it by independent measurements. The AlGaN/GaN HEMT (10×125 μm) on wafer is developed at the Xidian University and measured for DC and AC characteristics. Figure 4 shows the cross section of the device. The undoped AlGaN/AlN/GaN heterostructure layers are grown on a 2-inch (1 inch = 2.54 cm) 4H–SiC substrate by metal–organic chemical vapor deposition (MOCVD). Next, a 100-nm thick AlN nucleation layer is deposited. Then, a 1.6-μm thick GaN buffer layer is grown, followed by a 1-nm AlN interlayer and a 20-nm thick undoped AlGaN barrier layer. Hall measurements show a sheet carrier density of 1.3×10^{13} cm^{-2} and an electron mobility of 1750 cm^2/V·s. The sheet resistance is approximately 300 Ω/□ at room temperature. Isolation is realized by Cl_2-based dry etching with a depth of 150 nm. Ti/Al/Ni/Au source and drain electrodes are then formed by electron-beam evaporation and annealed at 870 °C for 30 s. SiN passivation is achieved with plasma-enhanced chemical vapor deposition (PECVD) and its thickness is 60 nm. The gate recess was achieved by plasma etching. The gate footprint ($L_{\rm g} = 0.4$ μm) is opened by etching SiN using CF_4 plasma. Next, the Schottky gate was formed by Ni/Au/Ni. The gate–gate, gate–source, and gate–drain spacings are 40 μm, 0.7 μm, and 2.8 μm, respectively.

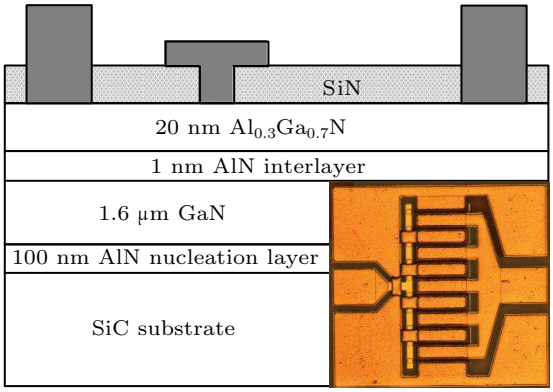


Fig. 4. (color online) Structure and photograph of the GaN FET.

We model the device following the extraction procedure we presented above. The values of extrinsic and linear intrinsic elements are shown in Fig. 1. The extracted DC, AC, and kink effect parameters are shown in Table 1.

The performance of the improved EEHEMT model with the kink effect is validated by comparing the fitting results of the *I–V* characteristics with the results of the original model.

The DC characteristics of the 1.25-mm-wide device are measured with the value of V_{ds} varying from 0 to 20 V in steps of 0.5 V and the value of V_{gs} changing from −3 V to 0.5 V in steps of 0.25 V. Figure 5(a) shows the comparison between the simulated results of the original EEHEMT model and the measured results. It indicates that in the high voltage area, the model fits to the measured curve well. However, in the kink effect domain, the disagreement between the simulated and measured results is obvious. Figure 5(b) shows the fitting results of the improved EEHEMT model with the kink effect. As can be seen, an excellent fitting is obtained for the entire bias range.

Table 1. Values of extracted DC, AC, and kink effect fitting parameters.

DC / AC / Kink effect								
DC	Gmmax/S	V_{go}/V	V_{co}/V	V_{to}/V	ALPHA/V	DELTGM/V^{-1}	V_{ba}/V	V_{bc}/V
	0.32	−2.05	−1.55	−2.9	0.01	0.05	0.5	1.5
AC	C11o/pF	C11th/pF	Vinfl/V	Deltgs/V	Deltds/V	Lambda/V^{-1}	C12sat/fF	Cgdsat/fF
	4.89	1.0	−2.43	1	0.01	0.005	110.6	250.0
Kink effect								
a_I	b_I	c_I	a_V	b_V	c_V	a_k	b_k	c_k	α
−0.007	−0.013	0.017	−0.8	−1.114	2.568	0.671	2.025	7.329	2.65

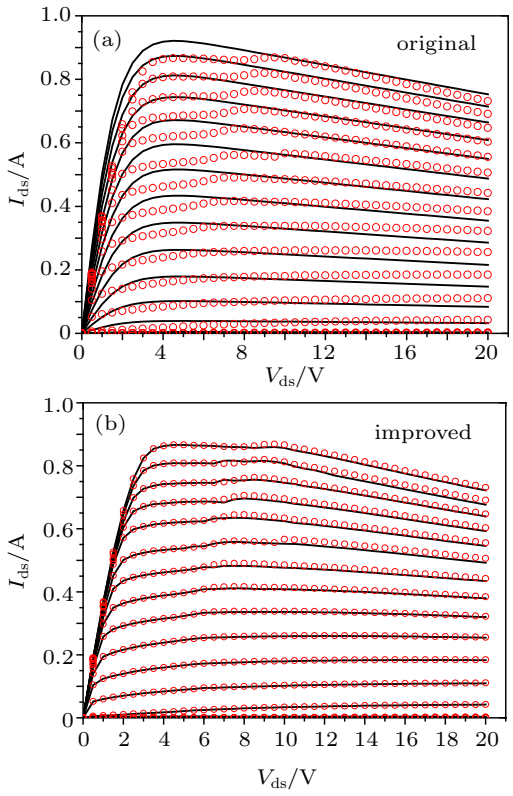


Fig. 5. (color online) Simulated (lines) and measured (circles) DC *I*–*V* characteristic results of (a) the original EEHEMT model and (b) the improved EEHEMT model.

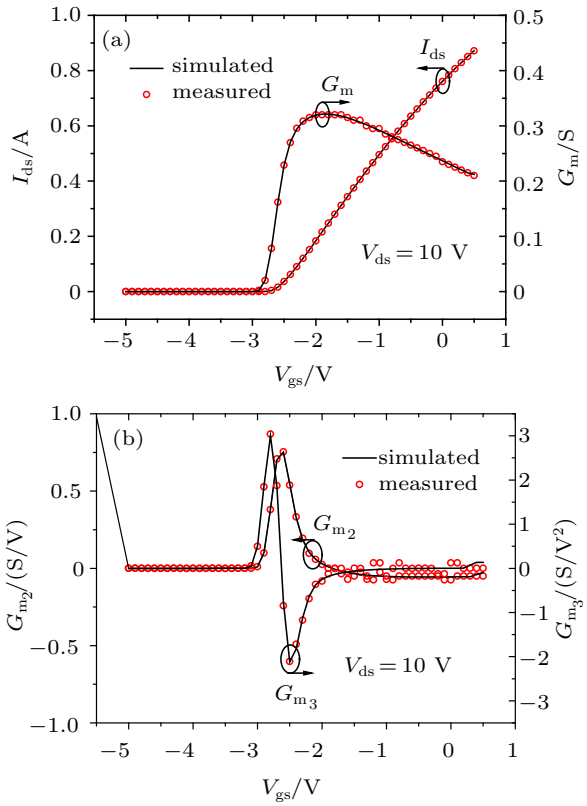


Fig. 6. (color online) Simulated (lines) and measured (circles) *I*–*V* characteristic and its first three derivatives, where (a) shows the *I*–*V* and G_m characteristics, and (b) shows the G_{m_2} and G_{m_3} characteristics.

To verify the DC accuracy of the model, we measure the transfer characteristics of the device and calculate its first three derivatives. Then we compare the simulated data of the improved model with the measured data. Figure 6 shows the comparison of the simulated and measured I_{ds}–V_{gs} curve and its first three derivatives (G_m, G_{m_2}, and G_{m_3}). Good agreement between the simulated and measured curves is obtained, which implies that the improved model is able to predict the DC behavior of the device accurately.

The original model and improved model *S*-parameter simulation results are compared with the measurements for a 1.25-mm gate width device, and the results are shown in Fig. 7 to validate the RF accuracies of the models. The good agreement between the measured small signal characteristic at $V_{gs} = -2$ V and $V_{ds} = 20$ V and both of the simulated results is obtained from 100.0 MHz to 26.5 GHz. This is because the DC and AC parameters of the EEHEMT model are extracted separately; kink parameters have no effect on the RF charac-

teristics of the model.

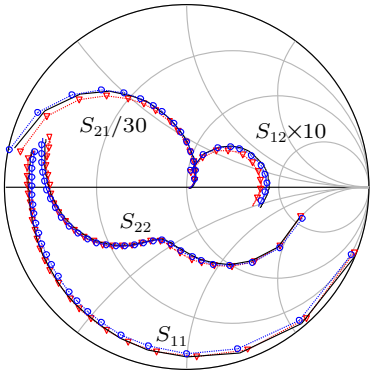


Fig. 7. (color online) *S*-parameter values obtained from the original model (circles), improved model (lines), and measurement (triangles) AlGaN/GaN HEMT (10×125 μm) on wafer at $V_{gs} = -2$ V and $V_{ds} = 20$ V in a frequency range from 100.0 MHz to 26.5 GHz.

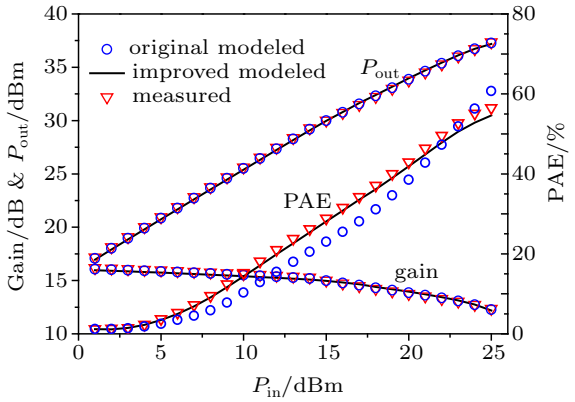


Fig. 8. (color online) Comparison of both the original and improved models simulated results with the measured results of output power, gain, and power-added efficiency (PAE) for a 1.25-mm-wide device at 5 GHz and $I_{dsq} = 100$ mA at bias voltage $V_{ds} = 28$ V.

The model is finally validated by simulating the large signal behavior of the 1.25-mm-wide device at 5 GHz and $I_{dsq} = 100$ mA at bias voltage $V_{ds} = 28$ V. The actual measurement is carried out with a load-pull system. Figure 8 shows the comparison of both the original and improved models simulated results with the measured output power, gain, and power-added efficiency (PAE) of the 1.25-mm-wide device. According to the comparison, it can be seen that both the original and the improved EEHEMT models describe the output power and gain of the device accurately. The improved model simulated PAE more accurately than the original one due to the improvement of the *I*–*V* characteristics simulation.

5. Conclusion

In this paper, an improved EEHEMT model for AlGaN/GaN HEMTs is presented. In this model, we propose a new current expression based on both the DC characteristics of the AlGaN/GaN HEMT and the hyperbolic tangent function tanh to describe the kink effect. We summarize the procedures to extract DC, AC, and kink effect parameters of the model and carry it out on a self-developed AlGaN/GaN HEMT with ten gate fingers each being 0.4-μm long and 125-μm wide. The improved model simulates the kink effect accurately while the simulated DC, *S*-parameters, and large-signal characteristics are in excellent agreement with the measured data.

References

[1] Kumar V, Lu W, Schwindt R, Kuliev A, Simin G, Yang J, Khan M A and Adesida Ilesanmi. 2002 *IEEE Electron Dev. Lett.* **23** 455
[2] Gaska R, Chen Q, Yang J, Osinsky A, Khan M A and Shur M S 1997 *IEEE Electron Dev. Lett.* **18** 492
[3] Wu Y F, Moore M, Saxler A, Wisleder T and Parikh P 2006 64*th Device Research Conference*, June 26–28, 2006, State College, Pennsylvania, USA, p. 151
[4] Quan S, Hao Y, Ma X H and Yu H Y 2011 *Chin. Phys. B* **20** 018101
[5] Yang L, Hu G Z, Hao Y, Ma X H, Quan S, Yang L Y and Jiang S G 2010 *Chin. Phys. B* **19** 047301
[6] Ma X H, Ma J G, Yang L Y, He Q, Jiao Y, Ma P and Hao Y 2011 *Chin. Phys. B* **20** 067304
[7] Enoki T, Kobayashi T and Ishii Y *IEEE* GaAs *IC Symp., Technical Digest* 1994, 16th *Annual*, Ocotober 16–19, 1994, Philadelphia, Pennsylvania, USA, p. 337
[8] Ma J G, Ma X H, Zhang H L, Cao M Y, Zhang K, Li W W, Guo X, Liao X Y, Chen W W and Hao Y 2012 *Acta Phys. Sin.* **61** 047301 (in Chinese)
[9] Anwar J and Gunter K 2007 *IEEE International Conference on Signal Processing and Communications*, 2007 ICSPC, November 24–27, 2007, Dubai, United Arab Emirate (UAE) p. 77
[10] Anwar J and Gunter K 2005 *IEEE Transactions on Microwave Theory and Techniques* **53** 3440
[11] Qi D X, Zhang Y T, Ning J X and Xu J F 2011 *Acta Mech. Solida Sin.* **24** 166